Surface & Coatings Technology 312 (2017) 61–65

Contents lists available at ScienceDirect

Surface & Coatings Technology

journal homepage: www.elsevier.com/locate/surfcoat

Nitrogen incorporation during PVD deposition of TiO_2:N thin films

Darina Manova [a,*], Lina Franco Arias [b], Axel Hofele [b], Ivo Alani [b], Ariel Kleiman [b], Iglika Asenova [a,c], Ulrich Decker [a], Adriana Marquez [b], Stephan Mändl [a]

[a] Leibniz-Institut für Oberflächenmodifizierung, Permoserstr. 15, 04318 Leipzig, Germany
[b] Instituto de Física del Plasma, CONICET and Departamento de Física, FCEN, Universidad de Buenos Aires, Cdad. Universitaria Pab. 1, 1428 Buenos Aires, Argentina
[c] Faculty of Physics, Sofia University "St. Kliment Ohridski", 5 James Bourchier Blvd, 1164 Sofia, Bulgaria

ARTICLE INFO

Article history:
Received 1 April 2016
Revised 17 August 2016
Accepted in revised form 27 August 2016
Available online 31 August 2016

Keywords:
TiO_2
PVD
Tauc plot
Band gap engineering

ABSTRACT

TiO_2:N is known for its photoactivity upon illumination with visible light. Using filtered arc with energetic particle fluxes, deposition near room temperature on sensitive substrates, e.g. polymers should be possible. However, addition of nitrogen gas flux during deposition results in very small nitrogen contents. Incorporation of nitrogen up to 5–7.5 at.% for either cathodic arc deposition or plasma based ion implantation and deposition leads to a reduction of the band gap down to 2.7 eV before the films become semimetallic. However, only deposition at a temperature of 200 °C allows avoiding the early formation of defects within the band gap. The nitrogen content was determined using secondary ion mass spectroscopy (SIMS) and calibrated with nitrogen implanted TiO_2 samples using conventional beamline implantation. The results show that the nitrogen/oxygen flow ratio in two completely different deposition systems is a reliable indicator of the physical properties.

1. Introduction

Titanium dioxide is well known as a photoactive material to be activated under UV irradiation [1,2] and employed either as a photocatalyst or exhibiting superhydrophilic after reducing the surface energy under illumination for self-cleaning or anti-fogging surfaces [3]. In addition to powders, TiO_2 can be produced as thin films using chemical sol-gel processes operating at air or physical vapour deposition (PVD) processes where either high temperature or increased ion energy is necessary to obtain an active phase [4]. Even coating of membranes is possible using a more complex process [5]. However, temperature sensitive substrates require low temperatures, ideally room temperature where an amorphous photoactive phase can be formed [6,7].

Independent of the phase composition the band gap is always more than 3 eV (the exact value depending on the polymorph), thus necessitating UV-A radiation for activation. For increasing the reactivity of the thin films, especially indoors, a reduced band gap is desired. Doping with transition metals or with nitrogen has been reported in the literature [8,9]. The latter dopant is – theoretically – readily accessible during PVD processes. However, the incorporation of nitrogen into the growing film, in contrast to ion implantation into TiO_2 thin films or selective oxidation of TiN, is a much more complex process which is presently not completely understood [10]. Alternatively, TiO_2 nanotubes with a reduced band gap [11], visible-light-active N-doped TiO_2 nanorods by hydrothermal treatment [12] or hydrazine doping of brookite nanorods at 200 °C for 18 h have been proposed recently [13].

In this report we utilize an energetic one-step PVD process for obtaining N-doped TiO_2 layers, which should allow the usage of temperature sensitive substrates. The deposition is performed for a range of backfill gas composition (oxygen and nitrogen) in order to investigate the influence of the total pressure and nitrogen/oxygen ratio on the film properties while comparing cathodic arc deposition (CAD) and plasma based ion implantation and deposition (PBIID). The resulting layers are subsequently investigated for correlation between their nitrogen content and optical properties. The aim is to optimise the nitrogen incorporation for band gap reduction while avoiding additional defects within the band gap and to investigate whether the process is suitable for transfer or scaling when assuming a future industrial application.

2. Experiment

Titanium dioxide thin films have been produced on Si and fused silica substrates using (a) cathodic arc deposition (CAD) in Buenos Aires and (b) plasma based ion implantation and deposition (PBIID) in Leipzig.

For the CAD samples, an arc current of 100 A was run between a pure Ti cathode (diameter 5.5 cm) and a stainless steel chamber that served as the anode. The cathodic arc system has been described in detail in a previous work [14]. A total gas flux (O_2 + N_2) of 54–65 sccm was used, the flow ratio N_2/O_2 being varied up to 2.2 and the working pressure resulting in around 5 Pa (at a base pressure of 0.01 Pa). Substrates

* Corresponding author.
E-mail address: darina.manova@iom-leipzig.de (D. Manova).

http://dx.doi.org/10.1016/j.surfcoat.2016.08.085
0257-8972/

were placed at a distance of 30 cm from the cathode surface on a grounded heater. For a process time of 120 s, films of 250–400 nm were obtained, deposition rates being in the range 2.1–3.3 nm/s. Besides samples without additional heating, reaching a substrate temperature of around 60 °C during the process, additional heating was employed for deposition at a substrate temperature of 200 °C.

The PBIID samples were produced in a 250-l cylindrical vacuum chamber with a base pressure better than 10^{-4} Pa, equipped with a vacuum cathodic arc [15]. The cathode was made of pure Ti (99.99%). The samples were mounted in the middle of the chamber at a distance to the cathode of 39 cm. The deposition experiments were performed under a flow of 50–60 sccm ($N_2 + O_2$) gas mixture, the flow ratio N_2/O_2 varying from zero up to 1. This resulted in a working pressure near 0.1 Pa. A constant arc current of 100 A was used, together with high voltage pulses of −3 kV at a pulse length of 30 μs and a repetition rate of 3 kHz (duty cycle 9%) for a treatment time of 300 s. The growth rate of slightly less than 1 nm/s resulted in films with a thickness of 250–300 nm. In addition to deposition at room temperature, i.e. without additional heating, deposition runs with auxiliary rf power (40.68 MHz) [16] or by heating the substrates to 200 °C from the backside using IR lamps [17] were performed.

For reference, pure TiO_2 samples at 60 sccm oxygen gas flow, stoichiometric TiN samples at 50 sccm nitrogen and substoichiometric TiN_x samples at 25 sccm nitrogen (termed $TiN_{0.5}$ in the following text) were produced on Si substrates. Additionally, beamline ion implantation was employed to implant 40 keV nitrogen ions into TiO_2 samples for fluences between 1 and 5×10^{17} cm^{-2}.

Analysis of the samples was performed using secondary ion mass spectroscopy (SIMS) in a time-of-flight setup with 15 keV $^{69}Ga^+$ primary ions for a scanned area of 100×100 μm^2. Sputtering for depth profiling was performed with 2 keV caesium ions, both incident at an angle of 45°. The secondary ion beam was scanned across 300×300 μm^2 to avoid crater edge effects. The surface region was analyzed by X-ray photoelectron spectroscopy (XPS) in order to obtain a confirmation of the nitrogen content independent of the SIMS calibration. However, as sputtering by Ar or coronene leads to a chemical reduction of the titanium oxide thin films with a subsequent systematic error in the composition [18], no depth profiling was attempted during the XPS measurements.

Optical properties of selected samples deposited on fused silica substrates were investigated with UV–visible spectroscopy (Shimadzu UV-1800). Transmission and absorption measurements were performed in the range 300–800 nm with a step size of 1 nm. Alternatively, measurements were taken (Agilent Cary 5000) in the range 200–800 nm with a step size of 1 nm. The optical band gap E_g of the films was calculated using the Tauc plot formalism for amorphous samples [19]. Plotting $(\alpha E)^{1/2}$ vs. E (with E photon energy and α absorption coefficient) leads to a straight line with the intercept defining the band gap [20].

3. Results & discussion

Before starting with the TiO_2:N samples, a method for estimating the nitrogen content within the films has to be established using the reference samples. Fig. 1 shows the SIMS data for the Cs_2N^+ cluster ion intensity, which was found to be representative for the nitrogen content in a previous experiment [10]. While the TiO_2 and TiN samples have been used for reference there, now the additional $TiN_{0.5}$ sample is measured, too. For the TiO_2 sample, some nitrogen is observed at the interface to the Si substrate. Both nitrogen containing Ti-N samples show identical count rates while the $TiN_{0.5}$ is metallic silver and clearly substoichiometric with massive nitrogen deficiencies [21]. While the nitrogen content clearly correlates with the cluster ion count rate, no linear, monotonically increasing relation between Ti and TiN exists. In contrast, a saturation level caused by matrix effects in SIMS should be present. As the previous publication [10] assumed a linear relation, the nitrogen content there is over estimated, albeit without consequences on the optical data presented there.

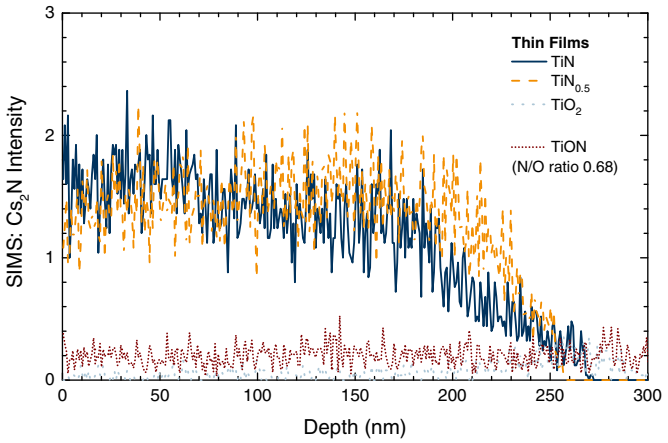

Fig. 1. SIMS Cs_2N^+ intensity for TiN, $TiN_{0.5}$ and TiO_2 reference samples on Si as function of depth. Additionally, data for a TiON samples produced at a N_2/O_2 flow ratio of 0.68 are shown.

For a more reliable calibration of the nitrogen content, 40 keV nitrogen ions were implanted in pure TiO_2 samples to different fluences between 1 and 5×10^{17} cm^{-2}. The expected nitrogen depth distributions have been calculated using SRIM [22]. For the low fluence of 1×10^{17} cm^{-2}, a very good agreement is observed for two separately implanted samples across the whole Gaussian profile – as shown in Fig. 2a – with no indication of any matrix effect. Hence, a single conversion factor for calculating the nitrogen concentration from the SIMS signal intensity was selected. When increasing the ion fluence to higher values (Fig. 2b and c), the same excellent agreement between both curves is observed only for low concentrations near the beginning and the end of the profile. For nitrogen concentrations beyond 10 at.%, the SIMS signal is already in saturation. Redistribution of the nitrogen may take place but will not explain the complete loss of concurrence between SRIM calculation and SIMS experiment. Thus, a saturation in SIMS is occurring around 10 at.% nitrogen in TiO_2. Up to this value, there is a linear relation between the nitrogen content and the SIMS signal intensity.

Keeping this limitation in mind, the nitrogen content of the films deposited by either CAD or PBIID has been determined from the SIMS data. The average value for the films – which show large variations in the nitrogen content only at the relatively high noise level – was used, except for the immediate surface and interface regions with additional contaminations or variations in the chemical composition being present there [23]. The corresponding results are plotted in Fig. 3 as a function of the nitrogen/oxygen flow ratios. As can be seen, the saturation level for the Cs_2N^+ signal in SIMS at 10 at.% nitrogen is never reached for the TiO_2:N thin films, even for very high N_2/O_2 flow ratios beyond 2. Concentrating first on the pure PBIID data (consisting of two separate data sets to check for consistency and reproducibility), a nearly linear relation between the nitrogen gas flow and the nitrogen content in the films is observed with 3 at.% being present for a flow ratio of 1:1. At this highest nitrogen concentration for this experiment, a semimetallic film is observed which is no longer transparent.

It is known that substoichiometric TiO_x films is a highly efficient getter material [24], thus an oxygen depleted atmosphere has to be present even for these low nitrogen contents to allow any nitrogen inside the films. As has been shown before, just adding nitrogen on top of the normal oxygen flow does result in no nitrogen incorporation at all [10]. Thus, alternative processing methods have been employed to assess whether a higher nitrogen content could be incorporated during the deposition phase.

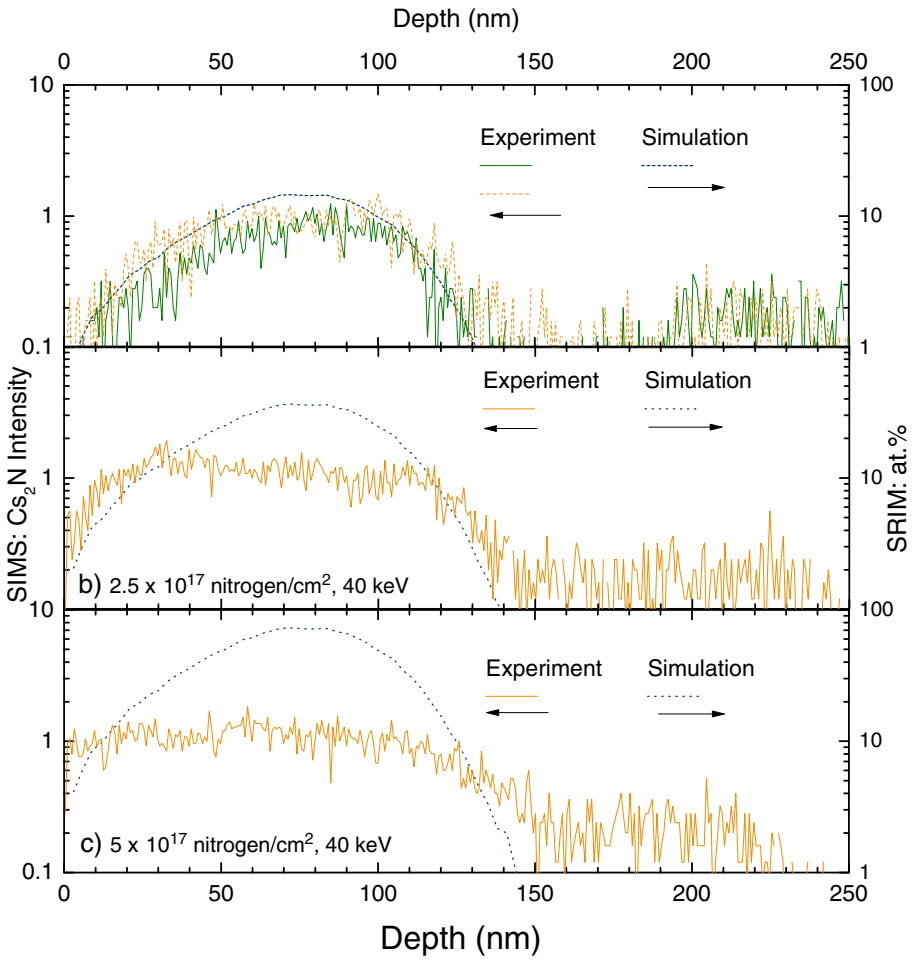

Fig. 2. SIMS Cs_2N^+ intensity compared with SRIM simulations for TiO_2 samples implanted with 40 keV nitrogen ions with different fluences.

Plasma activation by additionally providing an rf power of 150 W during the deposition run does not alleviate the situation: no increased nitrogen content and no increased transparency. Thus, additional nitrogen ions are not sufficient to lead to more nitrogen incorporation as apparently additional oxygen ions may increase the sputter rate and Ti—N bonds should be weaker than Ti—O bonds. However, heating the substrate to 200 °C during the deposition process results in a significant improvement of the nitrogen incorporation. The values of 3 at.% is now already found for a flow ratio of around 0.5 with a transparent film.

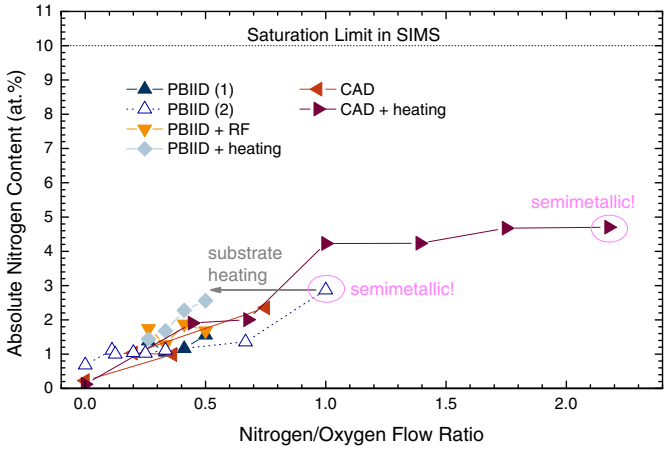

Fig. 3. Nitrogen content determined by SIMS as a function of the N_2/O_2 flow ratio for various batches of TiO_2:N samples, deposited by PBIID and CAD in different conditions. The different processing conditions are indicated. Unless stated, the films are transparent.

The CAD data show a similar picture, however the samples without heating have slightly higher nitrogen content than for PBIID at similar conditions. However, it has to be kept in mind that the substrate temperature without additional heating is actually slightly higher for CAD than for PBIID due to the more compact experimental design. When continuing the experiments to a massive nitrogen oversupply – at fixed pressure – a saturation of the nitrogen content with increasing nitrogen gas flow is observed even here near 4–5 at.% with a gradual transition towards semimetallic films at a flow ratio just beyond 2:1. This nitrogen content was confirmed by XPS studies for the surface region. As the samples are homogeneous according to the SIMS data, the quantification by SIMS and SRIM is supposedly correct. The saturation in the Cs_2N^+ count rate has only been observed for the reference samples and not for TiO_2:N films under investigation. Thus, the low SIMS count rate demonstrates that the nitrogen content in the TiO_2:N films is lower than 10 at.% for all investigated samples.

Influence of intermediate or higher temperatures have not been investigated at the moment. Nevertheless, the good agreement between two different experiments in Buenos Aires and Leipzig concerning the nitrogen content is regarded as an encouraging sign for transferring the obtained results to different systems or scaling the process towards industrial applications.

When looking at the optical properties, the transition from transparent towards semimetallic points in the direction of defect formation inside the band gap as the nitrogen content should be too low for an intermetallic compound similar to TiN with a band gap smaller than the visible light. Fig. 4 depicts the results obtained from the Tauc plots

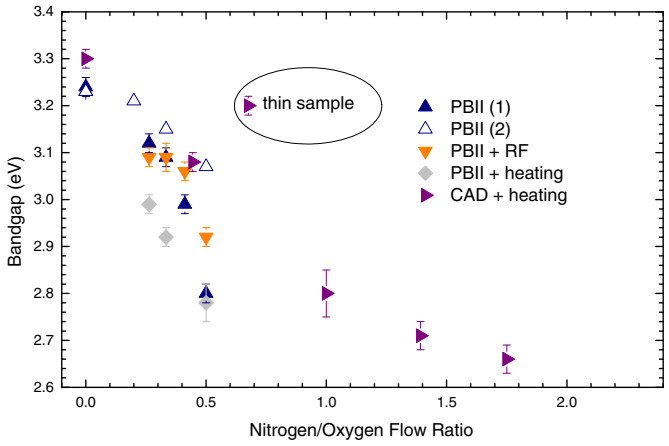

Fig. 4. Band-gap derived from Tauc plots assuming amorphous films as a function of the N_2/O_2 flow ratio for various batches of transparent TiO_2:N samples, deposited by PBIID and CAD in different conditions on fused silica substrates.

(for the transparent films only), again as a function of the nitrogen/oxygen flow ratio. For the PBIID data without heating a slow drop from about 3.3 to 3.0 eV is observed, while the samples heated during deposition show even lower values down to 2.6 eV. The value of the undoped TiO_2 corresponds to an amorphous phase. One value outside the general trend was observed for a thin sample where additional effects caused either by the substrate interface or the band gap determination may play a role.

A fair correlation between nitrogen content and band gap is visible in the data. Obviously, the main driving factor for reducing the band gap is the nitrogen incorporation and not any defect formation. It is assumed these defects are predominantly formed by the energetic ions impinging on the surface and being stopped within several monolayers. The underlying ion flux at constant pressure and plasma density should be also constant. Thus, the damage formation can be expected to be independent of the nitrogen/oxygen gas flow. The particle flux emanating from the arc (present in both experiments) is consisting of more than 99% ions with an average charge state of 2.03 [25], hence the energetic ion flux is actually by far the dominant contribution for the film growth.

Returning to the purported formation of defects within the band gap, transmission data for a selected series of PBIID samples are provided in Fig. 5. For the reference TiO_2 sample, well developed interference fringes due to the finite film thickness are observed, which are decreasing in amplitude with increasing nitrogen gas flow. The addition of rf

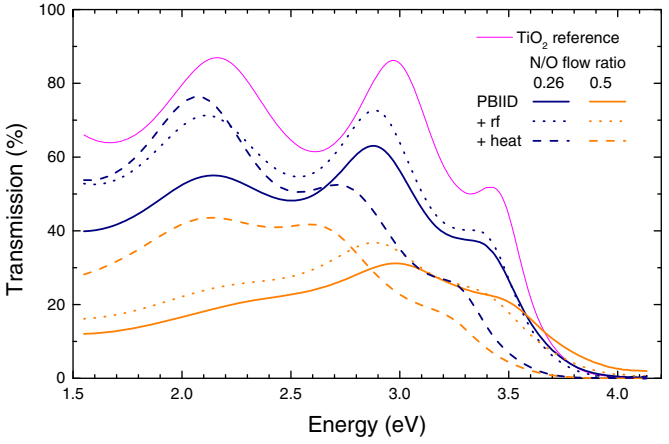

Fig. 5. Selected set of optical transmission spectra for TiO_2:N samples deposited by PBIID in different conditions: room temperature, with additional rf plasma activation and deposited at 200 °C.

power during the deposition process reverses this degradation of the films, i.e. increases defect density especially for very low nitrogen/oxygen gas flow ratios up to 0.41 but not for the curve measured for the highest value at 0.5. Thus, providing additional energy during the deposition process by increasing the plasma density and the ion bombardment is at least sufficient for the formation of defect states within the band gap but not for incorporating nitrogen itself. Similarly, a clear, positive effect for defect reduction is observed for maintaining the substrates at 200 °C during the deposition process, the films being more transparent and the transition to semimetallic being reached for higher nitrogen/oxygen flow ratios.

In general, doping of perfect single crystals leads to the formation of isolated defects within the band gap, which consequently morph into a defect band for higher concentrations. For anatase, theoretical calculations are available [26], showing that nitrogen incorporation leads to additional states about 0.13 eV above the valence band (while B and C lead to deep gap states), due to the substantial ionic character of anatase, additional states near 0.64 eV above the valence band edge are expected for nitrogen interstitial with a significant N—O bond. At the same time, electron trapping at Ti sites leads to the formation of Ti^{3+} defect states around 0.5–1.0 eV below the conduction band edge. Thus, nitrogen doping for anatase (single crystals) would lead to a favourable reduction of the band gap with the conduction band edge being still more positive than the reduction potential of H^+/H_2 [27].

For the present X-ray amorphous thin films, this argument is certainly not valid. Nevertheless, the local chemical order and constraints for bond angles and bond lengths should lead to similar energetic states as for single crystals [20]. Thus, it is assumed that the band gap reduction observed in the experiments is correlated with the addition of nitrogen related states near the valence band while additional gap states are due to disorder. Deposition of additional energy, e.g. by heating the substrate or more ion bombardment during the deposition process will anneal – at least partially – these defects [28]. Corresponding measurements are necessary to prove this hypothesis and to benefit from the theoretical modelling for further improvements in finding an optimum combination of activity and band gap reduction.

4. Summary & conclusions

Using PVD processes – CAD and PBIID – the successful formation of TiO_2:N thin films with a reduced band gap is reported. However substrate heating to 200 °C was necessary to achieve a reduced defect density within the band gap which otherwise leads to an early onset of the transition towards semimetallic films at 3 at.% nitrogen. At a concentration of 5 at.% a band gap of 2.65 eV is reported. However, this mandatory heating negates the purported advantages of deposition at room temperature. Further experiments are necessary to establish an upper limit for the necessary thermal load during deposition for high quality thin films. Additional experiments on the photocatalytic properties and their wavelength dependence are in progress.

Absolute nitrogen quantification using reference samples and comparison with XPS is possible for SIMS up to a concentration of 10 at.%. Good agreement was observed when comparing results from two disparate experimental setups where the nitrogen/oxygen gas flow provides a reliable indicator for the resulting film properties. Transfer and scaling of the process should thus be rather straightforward.

Acknowledgments

This study was partially supported by DFG grants for Initiation of International Collaborations (MA2054/16-1&MA2054/18-1) in conjunction with CONICET (Convocatoria 2012 CONICET – DFG para actividades de cooperación internacional). Frau Nadja Schönherr is acknowledged for conducting UV–VIS measurements in IOM Leipzig. Optical measurements were also performed at the Laboratorio de Polímeros y Materiales Compuestos (LP&MC, IFIBA-DF, FCEN, UBA).

References

[1] W. Hofmeister, E. Tillmanns, W.H. Bauer, Refinement of barium tetratitanate, $BaTi_4O_9$, and hexabarium 17-titanate, $Ba_6Ti_{17}O_{40}$, Acta Crystallogr. C 40 (1984) 1510–1512.

[2] A. Fujishima, K. Honda, Electrochemical photolysis of water at a semiconductor electrode, Nature 238 (1972) 37–38.

[3] R. Wang, K. Hashimoto, A. Fujishima, M. Chikuni, E. Kojima, A. Kitamura, M. Shimohigoshi, T. Watanabe, Light-induced amphiphilic surfaces, Nature 388 (1997) 431–432.

[4] P. Löbl, M. Huppertz, D. Mergel, Nucleation and growth in TiO_2 films prepared by sputtering and evaporation, Thin Solid Films 251 (1994) 72–79.

[5] K. Fischer, M. Kühnert, R. Gläser, A. Schulze, Photocatalytic degradation and toxicity evaluation of diclofenac by nanotubular titanium dioxide–PES membrane in a static and continuous setup, RSC Adv. 5 (2015) 16340–16348.

[6] J.M. Schneider, S. Rohde, W.D. Sproul, A. Matthews, Recent developments in plasma assisted physical vapour deposition, J. Phys. D. Appl. Phys. 33 (2000) R173–R186.

[7] D. Manova, A. Gjevori, F. Haberkorn, J. Lutz, S. Dimitrov, J.W. Gerlach, E. Valcheva, S. Mändl, Formation of hydrophilic and photocatalytically active TiO_2 thin films by plasma based ion implantation and deposition, Phys. Status Solidi A 206 (2009) 71–77.

[8] T. Morikawa, R. Asahi, T. Ohwaki, K. Aoki, Y. Taga, Band-gap narrowing of titanium dioxide by nitrogen doping, Jpn. J. Appl. Phys. 40 (2001) L561–L563.

[9] D.H. Lee, Y.S. Cho, W.I. Yi, T.S. Kim, J.K. Lee, H. Jin Jung, Metalorganic chemical vapor deposition of TiO_2:N anatase thin film on Si substrate, Appl. Phys. Lett. 66 (1995) 815–816.

[10] I. Asenova, D. Manova, S. Mändl, Incorporation of nitrogen into TiO_2 thin films during PVD processes, J. Phys. Conf. Ser. 559 (2014), 012008.

[11] B. Choudhury, S. Bayan, A. Choudhury, P. Chakraborty, Narrowing of band gap and effective charge carrier separation in oxygen deficient TiO_2 nanotubes with improved visible light photocatalytic activity, J. Colloid Interface Sci. 465 (2016) 1–10.

[12] S. Abu Bakar, G. Byzynski, C. Ribeiro, Synergistic effect on the photocatalytic activity of N-doped TiO_2 nanorods synthesised by novel route with exposed (110) facet, J. Alloys Compd. 666 (2016) 38–49.

[13] J. Pan, S.P. Jiang, Synthesis of nitrogen doped faceted titanium dioxide in pure brookite phase with enhanced visible light photoactivity, J. Colloid Interface Sci. 469 (2016) 25–30.

[14] A. Márquez, G. Blanco, M.E. Fernandez de Rap, D.G. Lamas, R. Tarulla, Properties of cupric oxide coatings prepared by cathodic arc deposition, Surf. Coat. Technol. 187 (2004) 154–160.

[15] G. Thorwarth, S. Mändl, B. Rauschenbach, Plasma immersion ion implantation using titanium and oxygen ions, Surf. Coat. Technol. 128 (129) (2000) 116–120.

[16] A. Gjevori, J.W. Gerlach, D. Manova, W. Assmann, E. Valcheva, S. Mändl, Influence of auxiliary plasma source and ion bombardment on growth of TiO_2 thin films, Surf. Coat. Technol. 205 (2011) S232–S234.

[17] A. Gjevori, K. Nonnenmacher, B. Ziberi, D. Hirsch, J.W. Gerlach, T. Höche, D. Manova, S. Mändl, Investigation of nucleation and phase formation of photocatalytically active TiO_2 films by MePBIID, Nucl. Instrum. Methods; B 267 (2009) 1658–1661.

[18] L. Soriano, M. Abbate, J. Vogel, J.C. Fuggle, A. Fernández, A.R. González-Elipe, M. Sacchi, J.M. Sanz, Chemical changes induced by sputtering in TiO_2 and some selected titanates as observed by X-ray absorption spectroscopy, Surf. Sci. 290 (1993) 427.

[19] J. Tauc, Absorption edge and internal electric fields in amorphous semiconductors, Mater. Res. Bull. 5 (1970) 721–730.

[20] E.A. Davis, N.F. Mott, Conduction in non-crystalline systems V. Conductivity, optical absorption and photoconductivity in amorphous semiconductors, Philos. Mag. 22 (1970) 903–922.

[21] P. Huber, D. Manova, S. Mändl, B. Rauschenbach, Optical characterization of TiN produced by metal-plasma immersion ion implantation, Surf. Coat. Technol. 142 (144) (2001) 418–423.

[22] J.F. Ziegler, M.D. Ziegler, J.P. Biersack, SRIM - the stopping and range of ions in matter, Nucl. Instrum. Methods B 268 (2010) 1818–1823.

[23] S. Heinrich, S. Schirmer, D. Hirsch, J.W. Gerlach, D. Manova, W. Assmann, S. Mändl, Comparison of ZrN and TiN formed by plasma based ion implantation & deposition, Surf. Coat. Technol. 202 (2008) 2310–2313.

[24] K. Nakajima, A. Fujiyoshi, Z. Ming, M. Suzuki, K. Kimura, In situ observation of oxygen gettering by titanium overlayer on $HfO_2/SiO_2/Si$, using high-resolution Rutherford backscattering spectroscopy, J. Appl. Phys. 102 (2007) 064507.

[25] A. Anders, Ion charge state distributions of vacuum arc plasmas: the origin of species, Phys. Rev. E 55 (1997) 969–981.

[26] C. Di Valentin, Trends in non-metal doping of anatase TiO_2: B, C, N and F, Catal. Today 206 (2013) 12–18.

[27] L. Yang, H. Zhou, T. Fan, D. Zhang, Semiconductor photocatalysts for water oxidation: current status and challenges, Phys. Chem. Chem. Phys. 16 (2014) 6810–6826.

[28] A. Anders, A structure zone diagram including plasma-based deposition and ion etching, Thin Solid Films 518 (2010) 4087–4090.